

Sensing-aided Uplink Channel Estimation for Joint Communication and Sensing

Xu Chen, *Member, IEEE*, Zhiyong Feng, *Senior Member, IEEE*, J. Andrew Zhang, *Senior Member, IEEE*, Zhiqing Wei, *Member, IEEE*, Xin Yuan, *Member, IEEE*, and Ping Zhang, *Fellow, IEEE*

Abstract—The joint communication and sensing (JCAS) technique has drawn great attention due to its high spectrum efficiency by using the same transmit signal for both communication and sensing. Exploiting the correlation between the uplink (UL) channel and the sensing results, we propose a sensing-aided Kalman filter (SAKF)-based channel state information (CSI) estimation method for UL JCAS, which exploits the angle-of-arrival (AoA) estimation to improve the CSI estimation accuracy. A Kalman filter (KF)-based CSI enhancement method is proposed to refine the least-square CSI estimation by exploiting the estimated AoA as the prior information. Simulation results show that the bit error rates (BER) of UL communication using the proposed SAKF-based CSI estimation method approach those using the minimum mean square error (MMSE) method, while at significantly reduced complexity.

Index Terms—Sensing-aided communication, 6G, joint communication and sensing, Kalman Filter.

I. INTRODUCTION

Joint communication and sensing (JCAS) is regarded as one of the most promising techniques for dealing with the spectrum congestion problem in the future 6G networks, achieving wireless communication and sensing using the same transmit signals [1]–[3]. The uplink (UL) JCAS estimates sensing parameters from the UL channel state information (CSI) [4]. Therefore, the CSI is highly related to the environment sensing information such as the angle-of-arrival (AoA), delay (or range), and Doppler frequency for the signals between the base station (BS) and the user. Moreover, the CSI estimation is critical for realizing reliable communications.

The least-square (LS) method has been widely utilized for channel estimation due to its low complexity [5]. Nevertheless, its low CSI estimation accuracy may result in a large signal-to-noise ratio (SNR) loss for communications. To deal with this problem, the minimum mean square error (MMSE) method was proposed to improve the CSI estimation accuracy. However, the high complexity makes it challenging to be utilized in real applications [6]. Recently, the deep neural

Xu Chen, Z. Feng, and Z. Wei are with Beijing University of Posts and Telecommunications, Key Laboratory of Universal Wireless Communications, Ministry of Education, Beijing 100876, P. R. China (Email: {chenxu96330, fengzy, weizhiqing}@bupt.edu.cn).

J. A. Zhang is with the Global Big Data Technologies Centre, University of Technology Sydney, Sydney, NSW, Australia (Email: Andrew.Zhang@uts.edu.au).

Ping Zhang is with Beijing University of Posts and Telecommunications, State Key Laboratory of Networking and Switching Technology, Beijing 100876, P. R. China (Email: pzhang@bupt.edu.cn).

X. Yuan is with Commonwealth Scientific and Industrial Research Organization (CSIRO), Australia (email: Xin.Yuan@data61.csiro.au).

Corresponding author: Zhiyong Feng

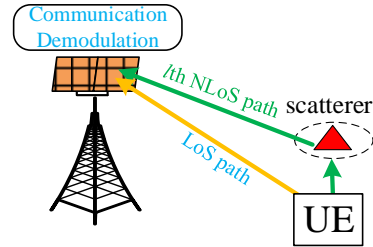


Fig. 1: The UL JCAS scenario.

network (DNN)-based estimation method was proposed [7]. By using the imperfect CSI to train the CSI estimation DNN, the CSI estimation can be improved. However, this method has high training overhead and thus is not suitable for real-time communication processing.

Exploiting the correlation between the sensing parameters and CSI, we propose a sensing-aided Kalman filter (SAKF)-based CSI estimation method for uplink (UL) JCAS. We propose a Kalman filter (KF)-based CSI enhancement method by exploiting the estimated AoA as the prior information to iteratively suppress the noise terms in CSI estimation. Simulation results show that the proposed SAKF-based CSI estimation method can achieve BER performance approaching that of the MMSE method, while at a significantly reduced complexity.

Notations: Bold uppercase letters denote matrices (e.g., \mathbf{M}); bold lowercase letters denote column vectors (e.g., \mathbf{v}); scalars are denoted by normal font (e.g., γ); the entries of vectors or matrices are referred to with square brackets; $(\cdot)^*$ and $(\cdot)^T$ denote Hermitian transpose, complex conjugate and transpose, respectively; $\mathbf{M}_1 \in \mathbb{C}^{M \times N}$ and $\mathbf{M}_2 \in \mathbb{R}^{M \times N}$ are $M \times N$ complex-value and real-value matrices, respectively; and $v \sim \mathcal{CN}(m, \sigma^2)$ means v follows a complex Gaussian distribution with mean m and variance σ^2 .

II. SYSTEM MODEL

We consider a UL JCAS system, where the BS and the user are equipped with uniform plane arrays (UPAs), as shown in Fig. 1. In the UL preamble (ULP) period, the user transmits the UL preamble signals, and BS receives them for CSI estimation, which is further used for estimating the sensing parameters, such as the AoAs, ranges and Doppler shifts. In the UL data (ULD) period, the BS receives and demodulates the UL data signals from the user using the estimated CSI.

Next, we introduce the transmit signal and received signal models.

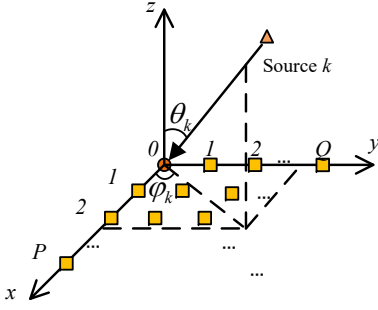


Fig. 2: The UPA model.

A. Transmit Signal Model

Orthogonal frequency division multiplexing (OFDM) signal is adopted as the transmit signal, which is given by

$$s(t) = \sum_{m=0}^{M_s-1} \sum_{n=0}^{N_c-1} \sqrt{P_t^U} d_{n,m} e^{j2\pi(f_c+n\Delta f)t} \text{Rect}\left(\frac{t-mT_s}{T_s}\right), \quad (1)$$

where P_t^U is the transmit power, M_s and N_c are the numbers of OFDM symbols and subcarriers, respectively; $d_{n,m}$ is the transmit OFDM baseband symbol of the m th OFDM symbol at the n th subcarrier, f_c is the carrier frequency, Δf is the subcarrier interval, $T_s = \frac{1}{\Delta f} + T_g$ is the time duration of each OFDM symbol, and T_g is the guard interval.

B. UPA Model

Fig. 2 demonstrates the UPA model. The uniform interval between neighboring antenna elements is denoted by d_a . The size of UPA is $P \times Q$. The AoA for receiving or the angle-of-departure (AoD) for transmitting the k th far-field signal is $\mathbf{p}_k = (\varphi_k, \theta_k)^T$, where φ_k and θ_k are the azimuth and elevation angles, respectively. The phase difference between the (p,q) th antenna element and the reference antenna element is

$$a_{p,q}(\mathbf{p}_k) = \exp[-j\frac{2\pi}{\lambda} d_a (p \cos \varphi_k \sin \theta_k + q \sin \varphi_k \sin \theta_k)], \quad (2)$$

where $\lambda = c/f_c$ is the wavelength of the carrier, f_c is the carrier frequency, and c is the speed of light. The steering vector for the array is given by

$$\mathbf{a}(\mathbf{p}_k) = [a_{p,q}(\mathbf{p}_k)]_{p=0,1,\dots,P-1;q=0,1,\dots,Q-1}, \quad (3)$$

where $\mathbf{a}(\mathbf{p}_k) \in \mathbb{C}^{PQ \times 1}$, and $[v_{p,q}]_{(p,q) \in \mathbf{S1} \times \mathbf{S2}}$ denotes the vector stacked by values $v_{p,q}$ satisfying $p \in \mathbf{S1}$ and $q \in \mathbf{S2}$. The sizes of the antenna arrays of the BS and the user are $P_t \times Q_t$ and $P_r \times Q_r$, respectively.

C. Received Signal Model

The frequency-domain received communication signal at the n th subcarrier of the m th OFDM symbol is expressed as [4]

$$\mathbf{y}_{C,n,m} = \sqrt{P_t^U} d_{n,m} \sum_{l=0}^{L-1} \begin{bmatrix} e^{j2\pi m T_s [f_{c,d,l} + \delta_f(m)]} \\ e^{-j2\pi n \Delta f [\tau_{c,l} + \delta_\tau(m)]} \\ \times b_{C,l} \chi_{TX,l} \mathbf{a}(\mathbf{p}_{RX,l}^U) \end{bmatrix} + \mathbf{n}_{t,n,m}, \quad (4)$$

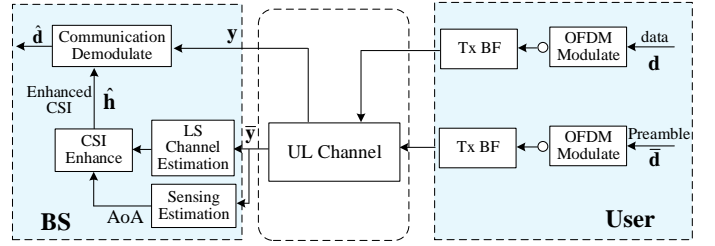


Fig. 3: The UL JCAS scheme with the SAKF-based CSI estimation.

where $l = 0$ is for the channel response of the LoS path, and $l \in \{1, \dots, L-1\}$ is for the l th non-LoS (NLoS) path; $\chi_{TX,l} = \mathbf{a}^T(\mathbf{p}_{TX,l}^U) \mathbf{w}_{TX}$ is the transmit BF gain, $\mathbf{w}_{TX} \in \mathbb{C}^{P_r Q_r \times 1}$ is the transmit beamforming (BF) vector, and $\mathbf{a}(\mathbf{p}_{TX,l}^U) \in \mathbb{C}^{P_r Q_r \times 1}$ and $\mathbf{a}(\mathbf{p}_{RX,l}^U) \in \mathbb{C}^{P_t Q_t \times 1}$ are the steering vectors for UL transmission and receiving, respectively; $f_{c,d,l}$ and $\tau_{c,l}$ are the Doppler and range of the l th path, respectively; $\delta_f(m)$ and $\delta_\tau(m)$ are the frequency and timing offsets, respectively; $b_{C,0} = 1$, $b_{C,l}$ ($l > 0$) is a random variable following $\mathcal{CN}(0, \sigma_{\beta_l}^2)$; $\mathbf{n}_{t,n,m}$ is the combined noise including Gaussian noise and possible reflected interferences, and each element of $\mathbf{n}_{t,n,m}$ follows $\mathcal{CN}(0, \sigma_N^2)$; and $\mathbf{y}_{C,n,m}$, $\mathbf{n}_{t,n,m} \in \mathbb{C}^{P_t Q_t \times 1}$. We adopt the low-complexity LS method to generate \mathbf{w}_{TX} , i.e., $\mathbf{w}_{TX} = [\mathbf{a}^T(\tilde{\mathbf{p}}_{TX,l}^U)]^\dagger$ [8], where $[\mathbf{A}]^\dagger$ is the pseudo-inverse matrix of \mathbf{A} . When the transmit beam alignment is complete, $\tilde{\mathbf{p}}_{TX,l}^U \approx \mathbf{p}_{TX,l}^U$. We denote the actual CSI as

$$\mathbf{h}_{C,n,m} = \sum_{l=0}^{L-1} \begin{bmatrix} e^{j2\pi m T_s [f_{c,d,l} + \delta_f(m)]} e^{-j2\pi n \Delta f [\tau_{c,l} + \delta_\tau(m)]} \\ \times b_{C,l} \sqrt{P_t^U} \chi_{TX,l} \mathbf{a}(\mathbf{p}_{RX,l}^U) \end{bmatrix}. \quad (5)$$

III. SAKF-BASED CSI ESTIMATION METHOD

In this section, we present the SAKF-based CSI estimation method. The UL JCAS scheme is shown in Fig. 3. In the ULP period, the UL CSI estimation at the n th subcarrier of the m th OFDM symbol is obtained with the LS method as [5]

$$\hat{\mathbf{h}}_{C,n,m} = \frac{\mathbf{y}_{C,n,m}}{d_{n,m}} = \mathbf{h}_{C,n,m} + \tilde{\mathbf{n}}_{t,n,m} \in \mathbb{C}^{P_t Q_t \times 1} \quad (6)$$

where $\mathbf{y}_{C,n,m}$ is given in (4), and $d_{n,m}$ is the preamble symbol with unit constant modulus. Since N_c subcarriers at M_s OFDM preamble symbols are used, we can stack all the CSIs to obtain the matrix $\hat{\mathbf{H}}_C \in \mathbb{C}^{P_t Q_t \times N_c M_s}$, where the $[(m-1)N_c + n]$ th column of $\hat{\mathbf{H}}_C$ is $\hat{\mathbf{h}}_{C,n,m}$.

In UL JCAS operation, the AoAs, ranges, and Dopplers are jointly estimated, as discussed in [9]. Specifically, the number of incident signals and their AoAs can be jointly estimated with the minimum description length (MDL)-based multiple signal classification (MUSIC) method [10]. Besides, the noise power can be estimated by averaging the last $P_t Q_t - L$ eigenvalues of $\hat{\mathbf{H}}_C (\hat{\mathbf{H}}_C)^H$ as $\hat{\sigma}_N^2$.

The AoA can be estimated once and used over multiple consecutive packets. According to (6), we can see that $\hat{\mathbf{h}}_{C,n,m} (\hat{\mathbf{h}}_{C,n,m})^H$ does not contain $e^{j2\pi m T_s [f_{c,d,l} + \delta_f(m)]} e^{-j2\pi n \Delta f [\tau_{c,l} + \delta_\tau(m)]}$. Therefore, the AoA estimation is not prominently affected by the frequency

and timing offset, while it is a challenging issue for estimating the range and Doppler [4]. Thus, AoA is the most suitable sensing parameter to refine the communication CSI. Next, we propose the KF-based CSI enhancement method that uses the estimated AoAs to refine the CSI estimation.

A. KF-based CSI Enhancement Method

Reshape $\hat{\mathbf{h}}_{C,n,m}$ and $\mathbf{h}_{C,n,m}$ into $\hat{\mathbf{H}}_{C,n,m}$ and $\mathbf{H}_{C,n,m} \in \mathbb{C}^{P_t \times Q_t}$, respectively. According to (4), if we treat the l th incident signal as the observing signal, then $[\hat{\mathbf{H}}_{C,n,m}]_{p,q}$ can be rewritten as

$$\begin{aligned} [\hat{\mathbf{H}}_{C,n,m}]_{p,q} &= [\mathbf{H}_{C,n,m}]_{p,q} + [\mathbf{I}_{n,m}^l]_{p,q} + n_{t,n,m}^{p,q} \\ &= \sqrt{P_t^U} \alpha_{n,m,l} e^{-j\frac{2\pi}{\lambda} d_a (p \cos \varphi_l \sin \theta_l + q \sin \varphi_l \sin \theta_l)} \\ &\quad + [\mathbf{I}_{n,m}^l]_{p,q} + n_{t,n,m}^{p,q}, \end{aligned} \quad (7)$$

where $\alpha_{n,m,l} = b_{C,l} e^{j2\pi m T_s \tilde{f}_{d,l,m}} e^{-j2\pi n \Delta f \tilde{\tau}_{l,m}} \chi_{TX,l}$, $\tilde{f}_{d,l,m} = f_{c,d,l} + \delta_f(m)$, $\tilde{\tau}_{l,m} = \tau_{c,l} + \delta_\tau(m)$, and $n_{t,n,m}^{p,q} = [\tilde{\mathbf{n}}_{t,n,m}]_{pQ_t+q}$. Moreover, $[\mathbf{I}_{n,m}^l]_{p,q}$ is the interference signals in other paths, and is expressed as

$$[\mathbf{I}_{n,m}^l]_{p,q} = \sqrt{P_t^U} \sum_{i=0, i \neq l}^{L-1} \alpha_{n,m,i} e^{-j\frac{2\pi d_a}{\lambda} (p \cos \varphi_i \sin \theta_i + q \sin \varphi_i \sin \theta_i)}. \quad (8)$$

According to (7), we can treat $[\hat{\mathbf{H}}_{C,n,m}]_{p,q}$ as the noisy observation of $[\mathbf{H}_{C,n,m}]_{p,q}$. The state transfer expressions of $\mathbf{H}_{C,n,m}$ in the p -axis and q -axis are expressed, respectively, as

$$[\mathbf{H}_{C,n,m}]_{p+1,q} = [\mathbf{H}_{C,n,m}]_{p,q} A_{P,l}, \quad (9)$$

$$[\mathbf{H}_{C,n,m}]_{p,q+1} = [\mathbf{H}_{C,n,m}]_{p,q} A_{Q,l}, \quad (10)$$

where $A_{P,l}$ and $A_{Q,l}$ are the transfer factors. Using the estimated $\hat{\mathbf{p}}_{RX,l}^U = (\hat{\varphi}_l, \hat{\theta}_l)$, we obtain the estimations of $A_{P,l}$ and $A_{Q,l}$ as

$$\hat{A}_{P,l} = e^{-j\frac{2\pi d_a}{\lambda} \cos \hat{\varphi}_l \sin \hat{\theta}_l}, \hat{A}_{Q,l} = e^{-j\frac{2\pi d_a}{\lambda} \sin \hat{\varphi}_l \sin \hat{\theta}_l}. \quad (11)$$

According to (9) and (10), each row and column of $\hat{\mathbf{H}}_{C,n,m}$ can be filtered by a KF filter to suppress the noise in (7). Let $\hat{\mathbf{h}}_C$ and $\bar{\mathbf{h}}_C$ denote a row or a column of $\hat{\mathbf{H}}_{C,n,m}$ and its filtered vector, respectively. The prior estimation of $[\hat{\mathbf{h}}_C]_p$ can be expressed as

$$[\hat{\mathbf{h}}_C]_p^- = [\hat{\mathbf{h}}_C]_{p-1} A, \text{ for } p \in \{1, \dots, P-1\}, \quad (12)$$

where $A = \hat{A}_{P,l}$ or $\hat{A}_{Q,l}$ when $[\hat{\mathbf{h}}_C]_p$ is a column or a row vector, respectively. Then, $[\bar{\mathbf{h}}_C]_p$ can be further updated as [11]

$$[\bar{\mathbf{h}}_C]_p = [\hat{\mathbf{h}}_C]_p^- + K_p([\hat{\mathbf{h}}_C]_p - [\hat{\mathbf{h}}_C]_p^-), \quad (13)$$

where K_p is the data fusion factor. Moreover, K_p is expressed as [11]

$$\begin{aligned} K_p &= (p_{w,p}^-)^* (p_{w,p}^- + \sigma_N^2)^{-1}, \\ p_{w,p}^- &= A p_{w,p-1} A^*, \\ p_{w,p} &= (1 - K_p) p_{w,p}^-, \end{aligned} \quad (14)$$

where σ_N^2 is the power of the interference-plus-noise, its estimation is $\hat{\sigma}_N^2$, and $p_{w,0}$ is the variance of initial observation. Based on (9) and (10), we obtain

$$p_{w,0} = \frac{1}{P} \sum_{p=0}^{P-1} |[\hat{\mathbf{h}}_C]_p(A)^{-p} - [\hat{\mathbf{h}}_C]_0|^2. \quad (15)$$

Algorithm 1: KF-based CSI Enhancement method

Input: The observation variance $\sigma_N^2 = \hat{\sigma}_N^2$; The transfer factor $A = \hat{A}_p$; The observation sequence $\hat{\mathbf{h}}_C = [\hat{\mathbf{H}}_{C,n,m}]_{:,q}$.

Output: Filtered sequence $\bar{\mathbf{h}}_C = [\bar{\mathbf{H}}_{C,n,m}]_{:,q}$.

Step 1: The dimension of $\hat{\mathbf{h}}_C$ is obtained as P ;

Step 2: $[\bar{\mathbf{h}}_C]_0 = [\hat{\mathbf{h}}_C]_0$;

Step 3: $p_{w,0} = \frac{1}{P} \sum_{p=0}^{P-1} |[\hat{\mathbf{h}}_C]_p(A)^{-p} - [\hat{\mathbf{h}}_C]_0|^2$;

Step 4:

for $p = 1$ to $P - 1$ **do**

$[\hat{\mathbf{h}}_C]_p^- = A[\bar{\mathbf{h}}_C]_{p-1}$;

$p_{w,p}^- = A p_{w,p-1} A^*$;

$K_p = (p_{w,p}^-)^* (p_{w,p}^- + \sigma_N^2)^{-1}$;

$[\bar{\mathbf{h}}_C]_p = [\hat{\mathbf{h}}_C]_p^- + K_p([\hat{\mathbf{h}}_C]_p - [\hat{\mathbf{h}}_C]_p^-)$;

$p_{w,p} = (1 - K_p) p_{w,p}^-$;

end

Step 5: for $p = P - 1$ to 1 **do**

$[\hat{\mathbf{h}}_C]_{p-1}^- = A^{-1}[\bar{\mathbf{h}}_C]_p$;

$p_{w,p-1}^- = A^{-1} p_{w,p} (A^{-1})^*$;

$K_p = (p_{w,p-1}^-)^* (p_{w,p-1}^- + \sigma_N^2)^{-1}$;

$[\bar{\mathbf{h}}_C]_{p-1} = [\hat{\mathbf{h}}_C]_{p-1}^- + K_p([\hat{\mathbf{h}}_C]_{p-1} - [\hat{\mathbf{h}}_C]_{p-1}^-)$;

$p_{w,p-1} = (1 - K_p) p_{w,p-1}^-$;

end

return $[\bar{\mathbf{h}}_C]_{n=0, \dots, N_c-1}$.

Based on (12), (13), (14), and (15), we propose the KF-based CSI enhancement method as shown in **Algorithm 1**. Note that we further add an inverse version of KF in **Step 5** to completely exploit the sensing information, where the transfer factor is updated as A^{-1} . By exploiting the estimated AoAs of JCAS as the prior information, **Algorithm 1** can suppress the noise terms in (7).

By using **Algorithm 1** to filter Q_t columns of $\hat{\mathbf{H}}_{C,n,m}$ in parallel with $\hat{A}_{P,l}$, we can obtain $\hat{\mathbf{H}}_{C,n,m}^{l,(1)}$. Further, we can also use **Algorithm 1** to filter the p th row of $\hat{\mathbf{H}}_{C,n,m}^{l,(1)}$ by replacing the input with $A = \hat{A}_{Q,l}$ and $\hat{\mathbf{h}}_C = [\hat{\mathbf{H}}_{C,n,m}^{l,(1)}]_{p,:}$. After filtering all P_t rows of $\hat{\mathbf{H}}_{C,n,m}^{l,(1)}$, we obtain $\hat{\mathbf{H}}_{C,n,m}^{l,(2)}$. After obtaining all the $\hat{\mathbf{H}}_{C,n,m}^{l,(2)}$ for $l = 0, \dots, L-1$, the aggregation of all L channel components is given by $\hat{\mathbf{H}}_{C,n,m}^{(2)} = \sum_{l=0}^{L-1} \hat{\mathbf{H}}_{C,n,m}^{l,(2)}$.

After being filtered by **Algorithm 1**, the noise term in the CSI estimation will be suppressed. Vectorize $\hat{\mathbf{H}}_{C,n,m}^{(2)}$ as $\hat{\mathbf{h}}_{C,n,m}^{(2)} = \text{vec}(\hat{\mathbf{H}}_{C,n,m}^{(2)}) \in \mathbb{C}^{P_t Q_t \times 1}$. Then, we can use $\hat{\mathbf{h}}_{C,n,m}^{(2)}$ to demodulate UL data signals with zero-forcing (ZF) receive BF [5].

B. Complexity Analysis

In this subsection, we analyze the complexity of the above SAKF-based CSI estimation and compare it with the LS and MMSE CSI estimation methods. The CSI estimation of the MMSE method can be expressed as [5]

$$\hat{\mathbf{h}}_{MMSE} = \mathbf{R}_{\text{hh}} [\mathbf{R}_{\text{hh}} + \hat{\sigma}_N^2 \mathbf{I}]^{-1} \hat{\mathbf{h}}_{C,n,m}, \quad (16)$$

where $\mathbf{R}_{\text{hh}} = E(\mathbf{h}_{C,n,m} \mathbf{h}_{C,n,m}^H)$.

Let $N = P_t Q_t$. The complexity of the LS method comes from the complex-value division, which is $\mathcal{O}(N)$. The MMSE method adds the matrix inverse and multiplication operations based on the LS method. Therefore, the complexity of the MMSE method is $\mathcal{O}(N^3)$. In contrast, the SAKF method adds scalar KF iterations with only two rounds of circulations and uses the estimated AoAs of JCAS without additional sensing processing. Thus, the complexity of the SAKF method for JCAS system is $\mathcal{O}(N + 2N) = \mathcal{O}(3N)$.

IV. SIMULATION RESULTS

In this section, we present the simulation results of the BERs using the proposed SAKF method, compared with the LS and MMSE methods. The simulation parameters are listed as follows.

The carrier frequency is set to 28 GHz [12], the antenna interval, d_a , is half the wavelength, the sizes of antenna arrays of the BS and user are $P_t \times Q_t = 8 \times 8$ and $P_r \times Q_r = 1 \times 1$, respectively, and the number of paths is $L = 2$. The subcarrier interval is $\Delta f = 480$ kHz, the subcarrier number is $N_c = 256$, and the bandwidth is $B = N_c \Delta f = 122.88$ MHz. The number of OFDM symbols used for simulation is $M_s = 64$. The variance of the Gaussian noise is $\sigma_N^2 = 4.9177 \times 10^{-12}$ W. The transmit power is determined according to the given SNR and σ_N^2 . UL SNR is defined as the SNR of each antenna element of BS. According to (4), the UL SNR is expressed as $\gamma_c = P_t^U \sum_{l=0}^{L-1} |b_{C,l} \chi_{TX,l}^U|^2 / \sigma_N^2$.

Fig. 4 demonstrates the BERs using the SAKF, LS, and MMSE methods under 4-QAM modulation. The required SNR to achieve the given BER for the SAKF method is about 1.8 dB lower than that for the LS method, but 0.2 dB higher than that for the MMSE method. This is because **Algorithm 1** filters the CSI estimated by the LS method exploiting the estimated AoAs.

Fig. 5 plots the BER curves using the SAKF and MMSE methods under 4-QAM and 16-QAM modulations. It can be seen that the BER performance of the proposed SAKF method can approach that of the MMSE method in both low and high QAM orders. The above results indicate that the proposed SAKF method can approach the MMSE method in BER performance with the significantly reduced complexity.

V. CONCLUSION

In this paper, we propose a SAKF-based UL channel estimation method for JCAS system. The KF exploits the AoAs estimated from preamble signals as the prior information to refine the LS CSI estimation. Simulation results show that the SNR required to achieve the given BER for the proposed SAKF method is about 1.8 dB lower than the LS method, and about 0.2 dB higher than the MMSE method.

REFERENCES

- [1] F. Liu, C. Masouros, A. Petropulu, H. Griffiths, and L. Hanzo, "Joint radar and communication design: Applications, state-of-the-art, and the road ahead," *IEEE Transactions on Communications*, June 2020.
- [2] Z. Feng, Z. Wei, X. Chen, H. Yang, Q. Zhang, and P. Zhang, "Joint Communication, Sensing, and Computation Enabled 6G Intelligent Machine System," *IEEE Network*, vol. 35, no. 6, pp. 34–42, Nov. 2021.

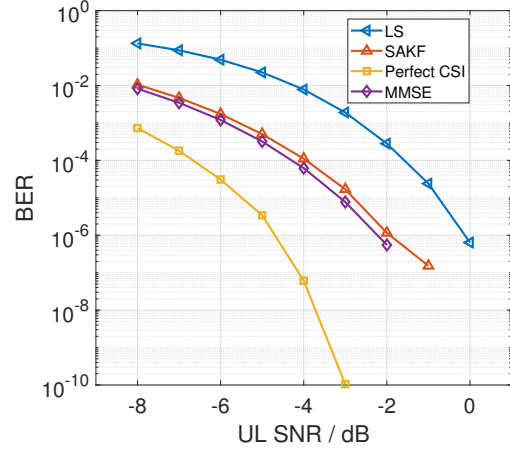


Fig. 4: The BERs using the SAKF, LS, and MMSE methods under 4-QAM modulation.

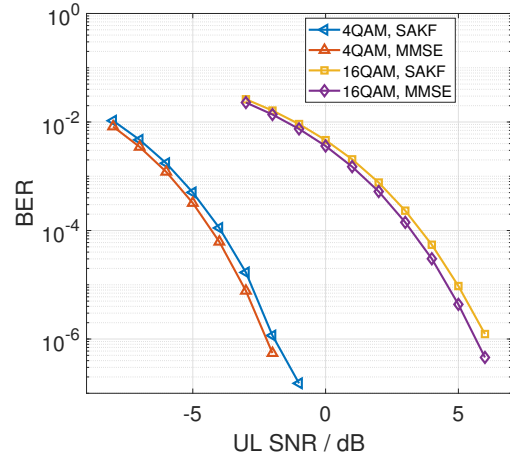


Fig. 5: The BERs using the SAKF and MMSE methods under 4-QAM and 16-QAM modulations.

- [3] W. Saad, M. Bennis, and M. Chen, "A Vision of 6G Wireless Systems: Applications, Trends, Technologies, and Open Research Problems," *IEEE Network*, vol. 34, no. 3, pp. 134–142, May 2020.
- [4] J. A. Zhang, K. Wu, X. Huang, Y. J. Guo, D. Zhang, and R. W. Heath, "Integration of radar sensing into communications with asynchronous transceivers," *IEEE Communications Magazine*, pp. 1–7, Aug. 2022.
- [5] Y. S. Cho, J. Kim, W. Y. Yang, and C. G. Kang, *MIMO-OFDM Wireless Communications with MATLAB*. Wiley Publishing, 2010.
- [6] W. H. T. Rodger E. Ziemer, *Principles of Communications*, 7th ed. Wiley, 2014.
- [7] L. Ge, Y. Guo, Y. Zhang, G. Chen, J. Wang, B. Dai, M. Li, and T. Jiang, "Deep neural network based channel estimation for massive mimo-ofdm systems with imperfect channel state information," *IEEE Systems Journal*, vol. 16, no. 3, pp. 4675–4685, 2022.
- [8] J. A. Zhang, X. Huang, Y. J. Guo, J. Yuan, and R. W. Heath, "Multibeam for joint communication and radar sensing using steerable analog antenna arrays," *IEEE Transactions on Vehicular Technology*, vol. 68, no. 1, pp. 671–685, Jan. 2019.
- [9] Z. Yang, R. Wang, Y. Jiang, and J. Li, "Joint estimation of velocity, angle-of-arrival and range (jevar) using a conjugate pair of zadoff-chu sequences," *IEEE Transactions on Signal Processing*, vol. 69, pp. 6009–6022, Oct. 2021.
- [10] Y. Gao, J. Xue, Y. Chang, and Y. Zhang, "An MDL-MUSIC joint time delay estimation method for LTE PRS," pp. 84–89, Oct. 2017.
- [11] G. C. Charles K. Chui, *Kalman Filtering: with Real-Time Applications*. Springer International Publishing, 2017.
- [12] "Study on evaluation methodology of new Vehicle-to-Everything V2X use cases for LTE and NR," *3GPP TR 37.885 V15.3.0*, 2019.